NUMERICAL STUDY OF THERMAL BEHAVIOR OF CONCRETE BRICKS USED IN LIBYA USING ANSYS SOFTWARE

Mohamed Salem, Khaled M. Sultan and Elfaitori Ibrahim

Mechanical Engineering Department, Omar Al-Mukhtar University, Libya
Email: mohamed.salem@omu.edu.ly

Received 1 April 2023, revised 25 June 2023, accepted 3 July 2023

الملخص

تم في هذا البحث، دراسة السلوك الحراري لثلاثة أنواع من طوب البناء الإسمنتي المستعمل في ليبيا حيث تم ذلك باستعمال المحاكاة العددية في وسط ثلاثي الابعاد. عند ظروف مستقرة، تم افتراض أن أحد أوجه الطوبة ساخن بينما الوجه الآخر بارد وكذلك ان درجات الحرارة ثابتة على كل من الأوجه. الهدف من هذه الدراسة هو مقارنة السلوك الحراري لثلاثة أنواع من طوب البناء التي يتم تصنيعها في ليبيا والتي تمتلك أبعادا وتجويفات بأحجام مختلفة عن طريق تحديد تأثير النسبة البعدية ورقم رالي على سلوك التدفق وانتقال الحرارة في التجويف. بينت هذه الدراسة أن رقم رالي يؤثر بشكل كبير على مظهر التدفق وانتقال الحرارة داخل التجويف وكذلك على سمك الطبقة الحرارية المتاخمة. لقد تم إثبات كذلك أن رقم نسلت يعتمد بشكل كبير على النسبة البعدية وان هذا المتغير اللابعدي يزداد بزيادة هذه النسبة. تم استعمال برنامج الانسس ووركبنتش اصدار 19.2 لأداء هذه المحاكاة والنمذجة.

ABSTRACT

In the present work, the thermal behaviour of three types of concrete bricks used in Libya was studied and analysed numerically in a three-dimensional computational domain. Under steady-state conditions, one side of the brick was assumed to be hot while the opposite side was assumed to be cold. Temperatures of the heated wall and of the cooled wall were assumed to be constant. The objective of this study is to compare the thermal behaviours of three types of concrete bricks manufactured and used in Libya that have different cavity sizes and different dimensions and determine the effects of the aspect ratio and Rayleigh number on flow behaviour and heat transfer in the cavity. This study showed that the Rayleigh number drastically influenced the flow profile and heat transfer inside the cavity, as well as the thickness of the thermal boundary layer. It was also verified that the Nusselt number is strongly dependent on the aspect ratio, and that this dimensionless variable increases with the increase of this ratio. ANSYS® Workbench™, version 19.2 has been used for modelling and simulation.

KEYWORDS: Natural Convection; Hollow Concrete Brick; Aspect Ratio; Rayleigh Number; Nusselt Number

INTRODUCTION

In Libya as well as in many other countries electric equipment, such as air conditioners and electrical heaters, have become indispensable in buildings for supplying thermally comfortable indoor environments. Consequently, the demand for electricity has increased sharply, particularly during the last few years with the increase in domestic load. In some local regions, the ambient air temperature could reach up to 40^{o}C during summer days and the exterior surfaces of the building, including roofs and external wall surfaces, could reach higher temperatures if they are directly exposed to solar radiation. In some other local regions, the ambient air temperature could reach -5^{o}C during winter days. The masonry walls and roofs are the surfaces that are mostly exposed to outdoor temperature and solar radiation. Therefore, decreasing the heat transfer through these

elements will result in minimizing heat loss in winter and heat gain in summer. If the desirable indoor temperature is 25^{o}C, then the temperature difference through the building envelopes in some local regions could reach 20^{o}C, which has great influence on the consumption of energy and therefore its cost.

Since energy generation in Libya is based on fuel, the fuel demand increases and the rate of air pollution due to the emission of CO_2 will also increase. The energy consumed by the electric equipment for thermal comfort could be reduced by minimizing the heat transfer between the exterior and interior surfaces of the buildings. There are several ways to design a well-insulated building. For example, double-skin walls with insulating materials contribute to some extent in decreasing the heat flow, but the insulation materials are not widely used because of their high cost. Since the thermal conductivity of concrete is much higher than that of air, the thermal conductivity can be significantly reduced by making cavities or air gaps in the concrete bricks.

Many studies have shown that different configurations of cavities inside hollow bricks can influence their thermal performance. Al-Tamimi et al. [1] conducted a numerical study to determine the optimum geometry of holes for concrete bricks that would increase the thermal resistance of the wall. They investigated 23 models of masonry concrete bricks with different configurations of holes. Their results showed that 51% hollow ratio could reduce the average inner surface temperature of the concrete brick by 7.18^{o}C. For bricks with the same hollow ratio, it was observed that the shape of holes plays a major part in reducing the thermal flow.

Bouchair [2] simulated heat transfer through hollow clay bricks, considering various numbers and sizes of cavities, and filling them with air or insulating solid materials such as cork and polystyrene. The results obtained have shown that a change in the configuration of cavities could increase the thermal performance of the hollow brick by 20%. The reduction of wall emissivity as well as the injection of insulating materials presented better results by canceling the radiative and convective effects.

In a similar study, Fioretti and Principi [3] performed a numerical study on heat transfer through clay hollow bricks. By varying the design and configurations of cavities, and using different emissivity, they showed that a low emissivity treatment in the cavity's wall can reduce the brick thermal transmittance, equaling it to the values obtained when the cavities are filled with polystyrene.

Svoboda and Kubr [4] numerically analyzed vertical heat flux passing through hollow masonry bricks. They perceived that heat transfer in a cavity heated from below is highly dependent on the cavity cross-section area and that the ratio between the transmittance calculated for vertical and horizontal direction is a function of the cavity dimensions and the heat flux direction.

Li et al. [5] performed a numerical study on heat transfer through multi-holed clay bricks. They evaluated the effects of radiation inside the cavities and the number of cavities in each direction. The results demonstrated that more cavities in the brick result in low radiation influence. They also concluded that a great number of cavities reduce the natural convection effect inside the bricks, making the conductivity of the solid material the most important aspect for thermal flow.

In general, studies have shown that different configurations of cavities inside hollow bricks can influence the thermal behaviour of the bricks. This is due to the interactions between conduction, convection, and thermal radiation caused by the hollow geometry. Thus, the objective of this study is to compare the thermal behaviours of three types of concrete bricks used in Libya that have different cavity sizes and different

external dimensions and determine the effects of the aspect ratio and Rayleigh number on flow behaviour and heat transfer in the cavity. Understanding the thermal behaviours of these three types of bricks could help us develop better thermal insulation for buildings by, for example, using double-skin walls or changing configurations of cavities inside hollow bricks

GEOMETRY AND BOUNDARY CONDITIONS

The external and internal dimensions for the studied bricks are shown in Figure (1). It shows the height H and length L of the rectangular cavities of all three bricks. Based on these dimensions, the aspect ratio (H/L) of the three cavities are 1.167, 1.75, and 3.5 for brick 20, brick 15, and brick 10, respectively. Out of the six external surfaces of the bricks, four were established as adiabatic, and two as isothermal. The temperature difference between the two parallel isothermal surfaces is varied from $\Delta T = 1$ K to $\Delta T =$ 13K, and keeping the hot surface temperature at $T_H = 294$K. This temperature difference assures laminar airflow inside the cavities. In this study, two processes of heat transfer were considered, which are conduction and convection. Pure conduction occurs through the solid part of the bricks, while the heat transfer by convection occurs through air cavities of the hollow bricks.

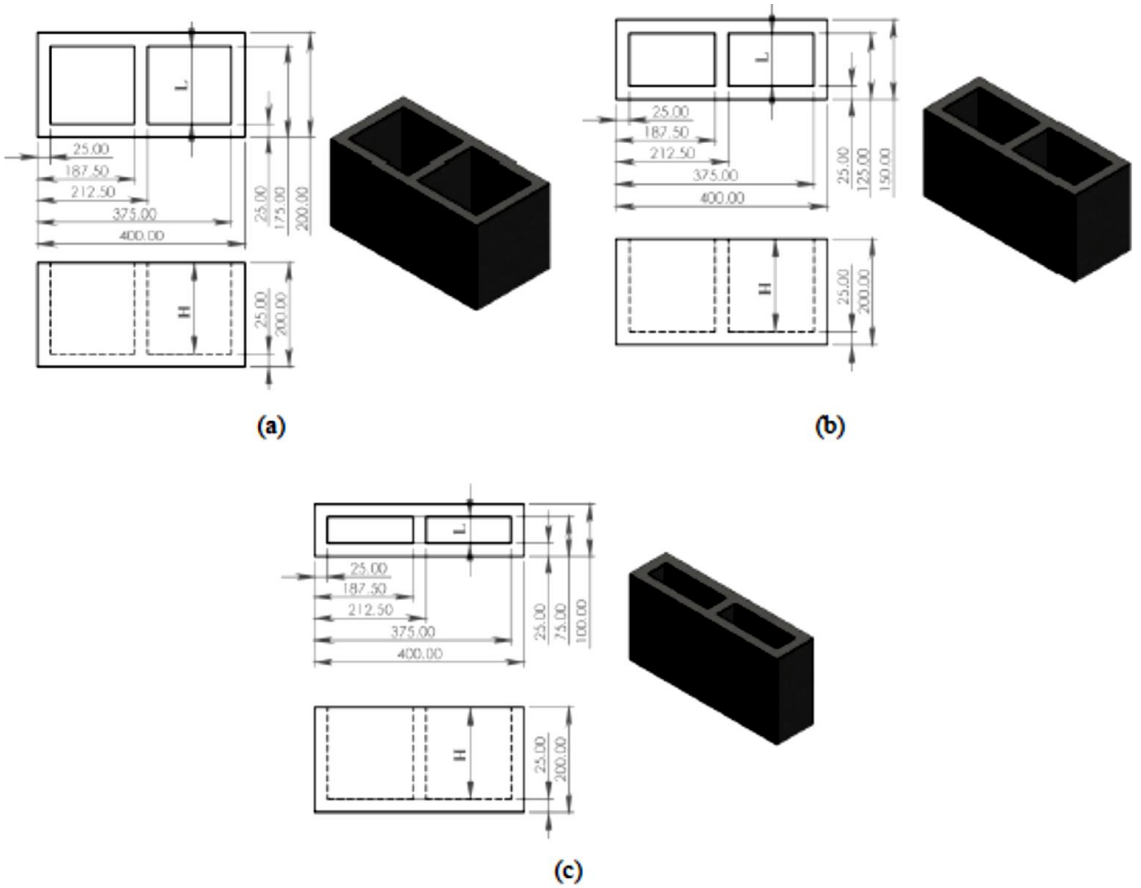

Figure 1: Geometric configurations of the three bricks (a) Brick 20 (B20), (b) Brick 15 (B15), (c) Brick 10 (B10). Dimensions are in mm.

SIMULATION PROCEDURE

All simulations were performed using ANSYS® Workbench™ software, version 19.2, choosing Fluent® Package. In this three-dimensional study, a structured mesh was

considered for each brick. The elements had a cubic form, with 2.4mm of edge length. All the simulations were performed considering steady-state heat transfer.

According to the literature [6], an internal flow is considered turbulent only when the Rayleigh number is higher than 10^9. The value of Rayleigh number inside the cavities of all bricks did not reach this limit. Thus, the air circulation inside each cavity, which promotes natural convection, was considered as a laminar flow, ruled by the following Navier-Stokes and energy equations. The full details of these equations can be also found in several other studies such as [6,7].

$$\frac{\partial u}{\partial x}+\frac{\partial v}{\partial y}+\frac{\partial w}{\partial z}=0 \tag{1}$$

$$\rho\left(u\frac{\partial u}{\partial x}+v\frac{\partial u}{\partial y}+w\frac{\partial u}{\partial z}\right)=-\frac{\partial p}{\partial x}+\mu\left(\frac{\partial^2 u}{\partial x^2}+\frac{\partial^2 u}{\partial y^2}+\frac{\partial^2 u}{\partial z^2}\right) \tag{2}$$

$$\rho\left(u\frac{\partial v}{\partial x}+v\frac{\partial v}{\partial y}+w\frac{\partial v}{\partial z}\right)=-\frac{\partial p}{\partial y}+\mu\left(\frac{\partial^2 v}{\partial x^2}+\frac{\partial^2 v}{\partial y^2}+\frac{\partial^2 v}{\partial z^2}\right)+\rho g \tag{3}$$

$$\rho\left(u\frac{\partial w}{\partial x}+v\frac{\partial w}{\partial y}+w\frac{\partial w}{\partial z}\right)=-\frac{\partial p}{\partial z}+\mu\left(\frac{\partial^2 w}{\partial x^2}+\frac{\partial^2 w}{\partial y^2}+\frac{\partial^2 w}{\partial z^2}\right) \tag{4}$$

$$\rho c_p\left(u\frac{\partial T}{\partial x}+v\frac{\partial T}{\partial y}+w\frac{\partial T}{\partial z}\right)=k\left(\frac{\partial^2 T}{\partial x^2}+\frac{\partial^2 T}{\partial y^2}+\frac{\partial^2 T}{\partial z^2}\right) \tag{5}$$

Where u is the velocity in x-direction, v is the velocity in y-direction, w is the velocity in z-direction, ρ is the density, p is the pressure, μ is the dynamic viscosity, c_p is the specific heat, and T is the temperature. Rayleigh number, Nusselt number, and convective heat transfer coefficient can be obtained by applying the following bench mark correlations [6],

$$Ra = Gr.Pr = \frac{g\beta(T_{H,i}-T_{C,i})L^3}{v^2}.Pr \tag{6}$$

$$\bar{N}u_L = 0.22\left(\frac{Pr}{0.2+Pr}Ra_L\right)^{0.28}\left(\frac{H}{L}\right)^{-1/4} \tag{7}$$

$$\begin{bmatrix} 2 \le (H/L) \le 10 \\ Pr \le 10^5 \\ 10^3 \le Ra_L \le 10^{10} \end{bmatrix}$$

$$\bar{N}u_L = 0.18\left(\frac{Pr}{0.2+Pr}Ra_L\right)^{0.29} \tag{8}$$

$$\begin{bmatrix} 1 \le (H/L) \le 2 \\ 10^{-3} \le Pr \le 10^5 \\ 10^3 \le \dfrac{Ra_L Pr}{0.2+Pr} \end{bmatrix}$$

$$\bar{N}u_L = \frac{hL}{k} \tag{9}$$

Where Gr is Grashof number, Pr is Prandtl number, g [m/s^2] is the acceleration of gravity, β [K^{-1}] is the expansion coefficient, $T_{H,i}$ [K] is the inner surface temperature of the hot wall, $T_{C,i}$ [K] is the inner surface temperature of the cold wall, L [m] is the distance between the two inner surfaces, v [m^2/s] is the kinematic viscosity, and $\bar{N}u_L$ is Nusselt number, h is the convective heat transfer coefficient [w/m^2.k], and H/L is the aspect ratio.

The aspect ratios for the studied bricks are 1.167, 1.75, and 3.5 for B20, B15, and B10 respectively.

Because of symmetry, only half of the brick was studied to save computational time. Mesh independence was conducted for the hollow bricks with the largest cavity (B20) at $\Delta T = 1$ K. Six mesh sizes were considered ranging from 2 to 9 mm to find out the optimum mesh size. The change of heat transfer rate through the brick B20 at $\Delta T = 1$ K with the number of nodes is shown in Figure (2). It can be seen from this figure that the number of nodes has a significant effect on the computational results. However, comparing the 1,229,460-node mesh with the 2,107,296-node mesh, obviously showed that increasing the number of nodes has no more than a 0.13% difference in the heat transfer rate (Q). Therefore, the optimum number of nodes 1,229,460 (or 614,730 for half of the brick) has been chosen for the simulation to save time and reduce errors. A mesh of the solid part of the hollow bricks (B20) of the ANSYS software is shown in Figure (3) to present the type of mesh used in this study.

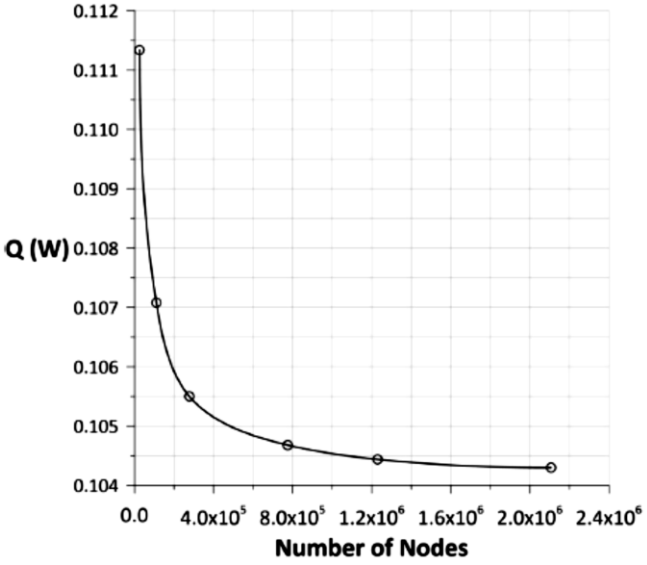

Figure 2: Grid dependence of the numerical results for B20 at $\Delta T = 1$ K

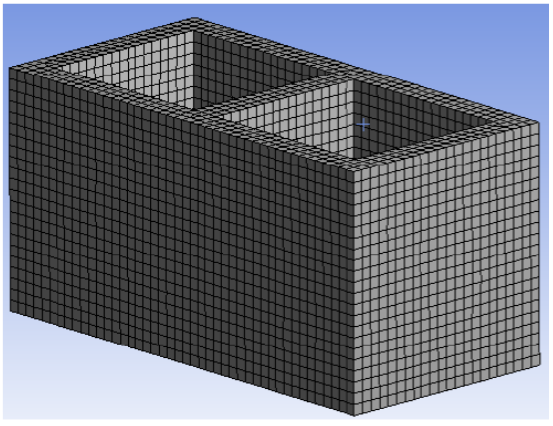

Figure 3: ANSYS meshing for B20

THERMAL PROPERTIES

Table (1) shows all the data of air properties needed in the simulation which were gathered from property tables [8]. The effective thermal conductivity of the solid material of the concrete brick was calculated using an averaged volume method based on averaging data of the materials (cement, aggregate, and sand) used by several local brick

manufacturers. The calculated value was k = 0.42 W/mK, which agrees well with the one found in the literature [9].

In Table (1), T_H (K) is the hot surface temperature, T_C (K) is the cold surface temperature, T_m (K) is the mean temperature, k (W/m.K) is the thermal conductivity of air, υ [m^2/s] is the kinematic viscosity, *Pr* is Prandtl number, c_p (J/kg.K) is the constant pressure specific heat, and β [K^{-1}] is the expansion coefficient.

Table 1: Air properties taken at the mean temperature

T_H (K)	T_C (K)	T_m (K)	k (W/m.K)	ν (m^2/s)	P_r	c_p (J/kg.K)	β (1/K)
294	293	293.5	0.0251	1.520×10^{-5}	0.7307	1007	0.0034
294	291	292.5	0.0251	1.511×10^{-5}	0.7310	1007	0.00341
294	289	291.5	0.0250	1.502×10^{-5}	0.7313	1007	0.00343
294	287	290.5	0.0249	1.493×10^{-5}	0.7316	1007	0.00344
294	285	289.5	0.0248	1.484×10^{-5}	0.7318	1007	0.00345
294	283	288.5	0.0247	1.474×10^{-5}	0.7321	1007	0.00346
294	281	287.5	0.0247	1.470×10^{-5}	0.7324	1006.9	0.00347

RESULTS AND DISCUSSIONS

The thermal behaviour for three types of local bricks is studied and analysed numerically in a three-dimensional computational domain. To verify the validity of the mesh used in this study, a comparison with benchmark results [10] was used for a cavity flow with Rayleigh number $Ra_L = 10^5$. As a pre-test, it was conceived as a cubic cavity with four adiabatic faces and two parallel isothermal faces. The pre-test was performed considering the same simulation procedures used for this study's bricks. Figure (4) shows the dimensionless temperature profile obtained in the pre-test and the benchmark solution. It can be clearly noticed the great similarity between the pre-test and the benchmark temperature profiles which validates the mesh used in this study.

Tables (2, 3, and 4) present the values of Rayleigh numbers, Nusselt numbers, and convective heat transfer coefficients calculated based on the numerically evaluated temperature difference values and the different geometries of the three bricks. The obtained data are also plotted in Figures (5 and 6).

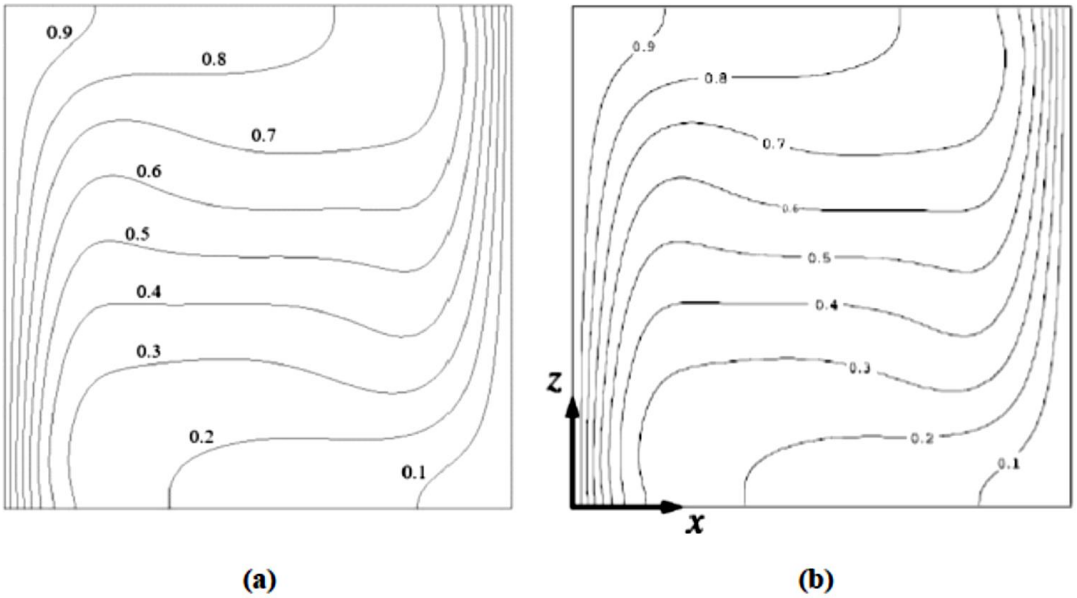

Figure 4: The dimensionless temperature profiles: (a) pre-test, (b) benchmark [10]

Based on most of the previous studies [11], the estimated value of the convection heat transfer coefficient inside the cavities is approximately 1.25 W/m^{2}K, which is close to the values obtained in this study. The longer the cavity length the higher the convection heat transfer coefficient value. This can be explained by the influence of higher velocities reached by the air inside the cavities. For example, at ΔT = 13 K, the maximum air velocities observed inside the cavities are 78, 74, 69 mm/s for B20, B15, and B10 respectively.

Table 2: Rayleigh number, Nusselt number, and heat transfer coefficient for B20

$T_{H,i}$ (K)	$T_{C,,i}$ (K)	Ra_L	$\bar{N}u_L$	h (W/m^2.K)
293.934	293.057	3.126×10^5	6.582	0.946
293.749	291.216	9.175×10^5	8.994	1.290
293.535	289.402	1.521×10^6	10.415	1.489
293.300	287.604	2.130×10^6	11.484	1.637
293.051	285.82	2.748×10^6	12.364	1.757
292.79	284.046	3.381×10^6	13.131	1.860
292.518	282.282	3.995×10^6	13.782	1.947

Table 3: Rayleigh number, Nusselt number, and heat transfer coefficient for B15

$T_{H,i}$ (K)	$T_{C,,i}$ (K)	Ra_L	$\bar{N}u_L$	h (W/m^2.K)
293.928	293.063	9.137×10^4	4.607	0.662
293.736	291.231	2.688×10^5	6.300	0.903
293.514	289.425	4.459×10^5	7.296	1.043
293.274	287.636	6.248×10^5	8.046	1.147
293.019	285.859	8.063×10^5	8.664	1.231
292.761	284.075	9.953×10^5	9.210	1.305
292.475	282.338	1.172×10^6	9.658	1.364

Table 4: Rayleigh number, Nusselt number, and heat transfer coefficient for B10

$T_{H,i}$ (K)	$T_{C,,i}$ (K)	Ra_L	$\bar{N}u_L$	h (W/m^2.K)
293.915	293.077	1.106×10^4	2.497	0.359
293.697	291.274	3.250×10^4	3.414	0.489
293.453	289.492	5.400×10^4	3.955	0.565
293.192	287.726	7.572×10^4	4.363	0.622
292.918	285.971	9.779×10^4	4.699	0.668
292.634	284.226	1.204×10^5	4.991	0.707
292.340	282.490	1.423×10^5	5.240	0.740

Data in Tables (2, 3, and 4) are also presented in Figures (5 and 6). Figure (5) shows the results of the calculated Rayleigh number for the three types of bricks as a function of the temperature difference between the inner surfaces of the hot and cold walls. It can be clearly observed that at any given temperature difference the Rayleigh number value of the B20 cavity is higher than those of B15 and B10. Hence, natural convection heat transfer, as expected, is most intense within the B20 cavity. It can also be noticed that the sharp divergence between the three curves and hence the intensity of natural convection is continuously widening with any increment of the temperature difference.

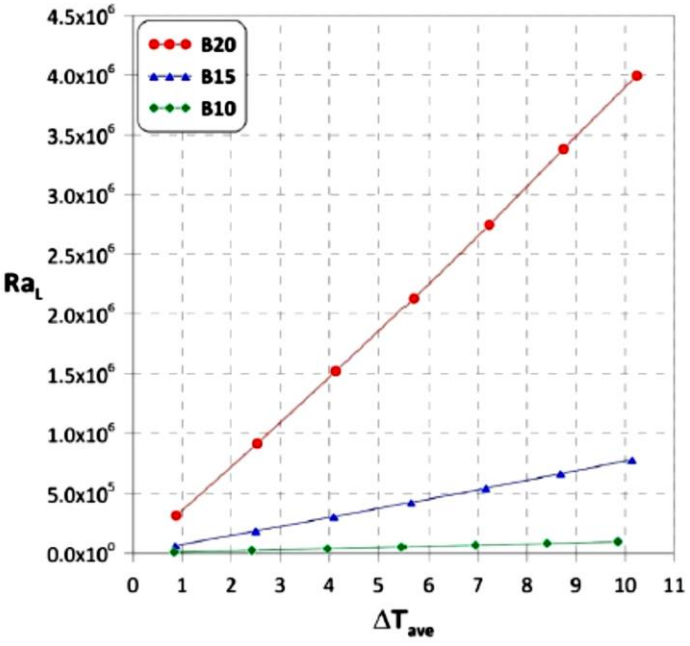

Figure 5: The change of Rayleigh number with the temperature difference between the inner surfaces of the hot and cold walls

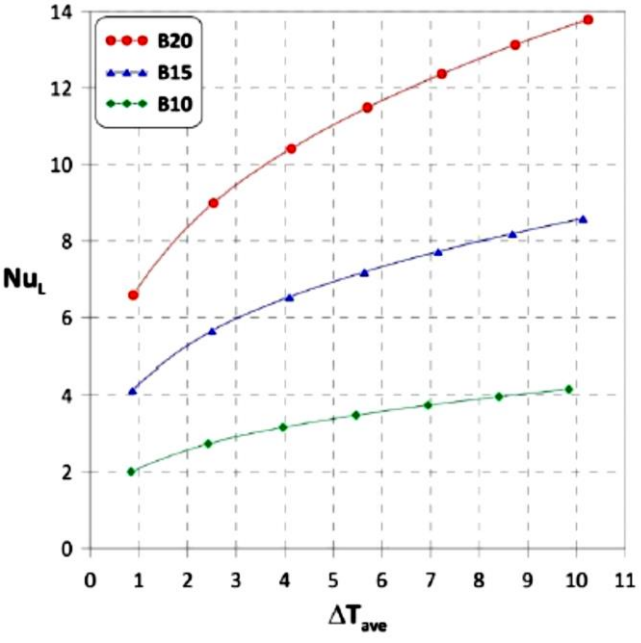

Figure 6: The change of Nusselt number with the temperature difference between the inner surfaces of the hot and cold walls

Figure (7) shows the numerically evaluated heat transfer rate values Q (W), versus the temperature difference ΔT (K) for the three studied bricks. It can be clearly noticed that even though natural convections as previously shown is the most intense inside the B20 brick, here the total heat transfer at any temperature difference values through this brick are the least. This is attributed to the conduction heat transfer which is less in the case of B20. As the width of the air gap decreases, the air circulation decreases and hence the natural convection also decreases and the conduction heat transfer becomes the dominant kind of the heat transfer within the air gap.

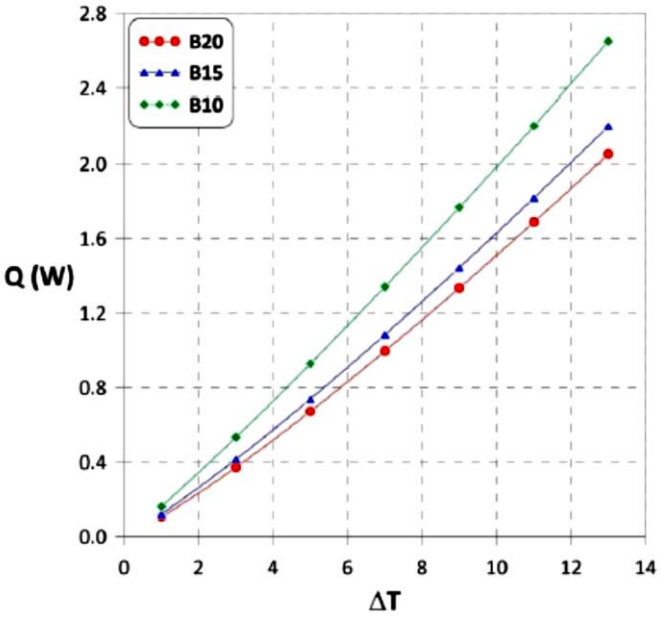

Figure 7: The change of heat transfer Q (W) with the temperature difference ΔT (K)

Figures (8-13) show the temperature contours and velocity vectors for the three bricks at the lowest and highest temperature difference considered in this study. They are taken in the middle of the cavity in the direction of heat transfer. These figures show the influence of Rayleigh number on the flow and heat transfer in the studied cavities. As shown by the velocity vectors, air motion is characterized by recirculating or cellular flow for which air ascends along the hot wall and descends along the cold wall. With increasing Rayleigh number, the cellular flow intensifies and becomes concentrated in thin boundary layers adjoining the sidewalls and the core becomes nearly stagnant.

Based on these figures it can be observed that in all cases studied as expected only one convection cell was formed for this range of Rayleigh numbers. The graphs of temperature contours show the formation of a thermal boundary layer along the hot and cold wall. The temperature gradient along the hot vertical wall for all cases is maximum at the top and decreases towards the bottom.

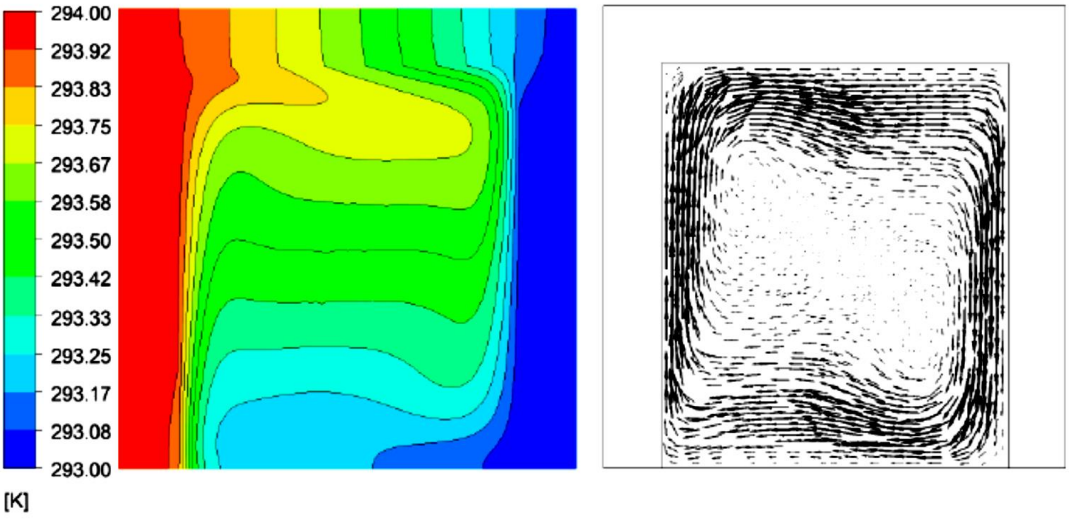

Figure 8: Temperature contours and velocity vectors for B20 at ΔT = 1 K ($Ra_L = 3.126\times10^5$)

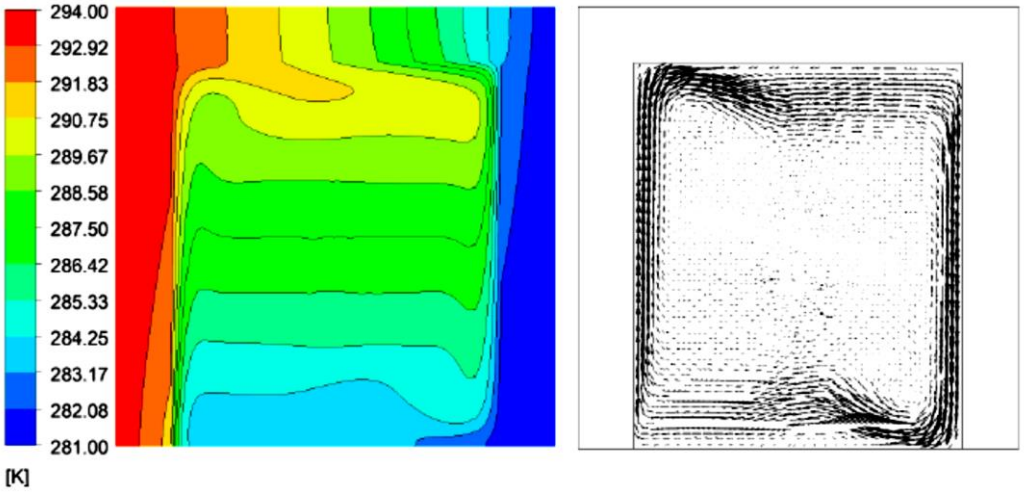

Figure 9: Temperature contours and velocity vectors for B20 at ΔT = 13 K ($Ra_L = 3.995\times10^6$)

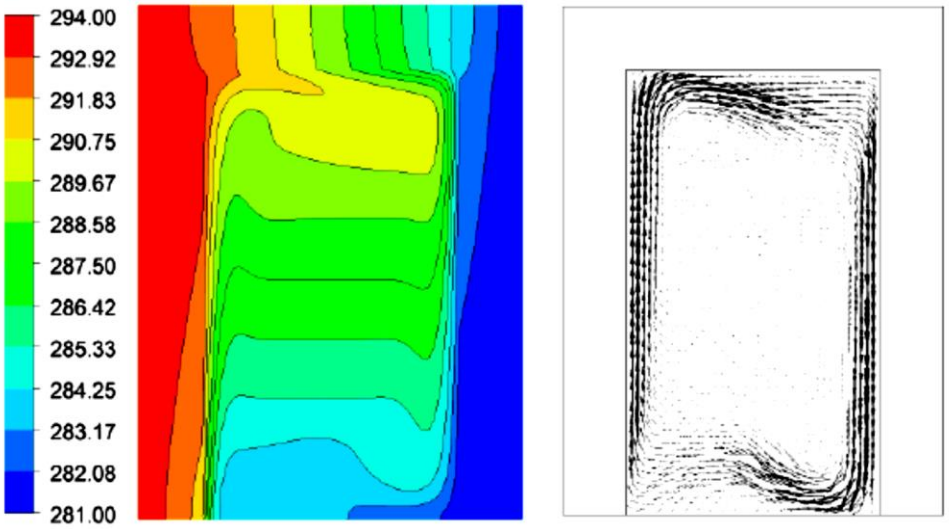

Figure 10: Temperature contours and velocity vectors for B15 at ΔT = 1 K ($Ra_L = 9.137\times10^4$)

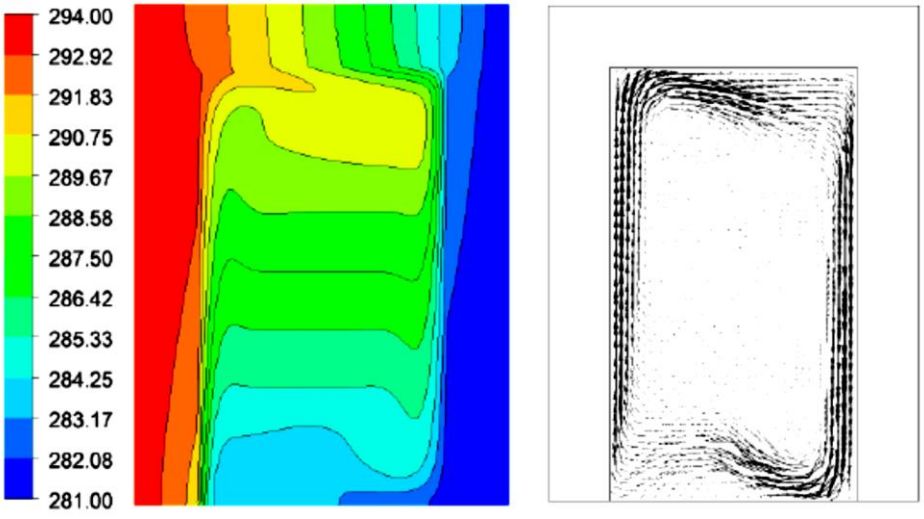

Figure 11: Temperature contours and velocity vectors for B15 at ΔT = 13 K ($Ra_L = 1.172\times10^6$)

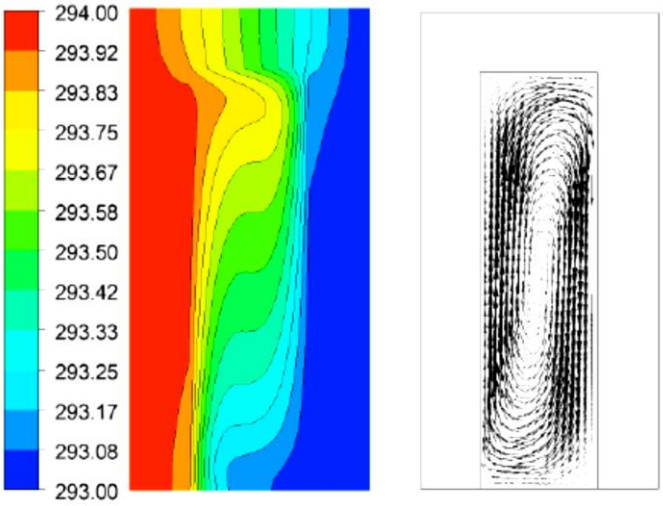

Figure 12: Temperature contours and velocity vectors for B10 at ΔT = 1 K ($Ra_L = 1.106\times10^4$)

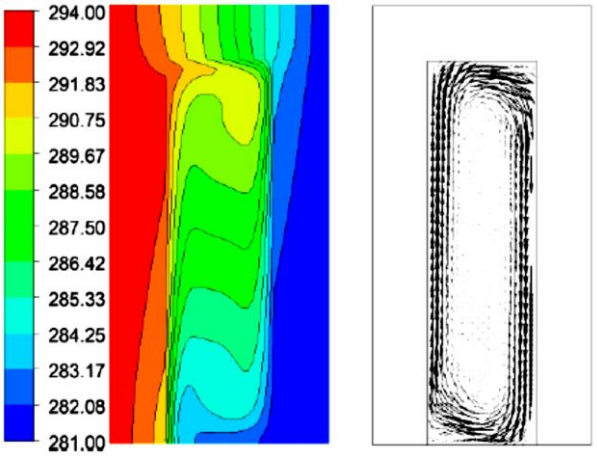

Figure 13: Temperature contours and velocity vectors for B10 at ΔT = 13 K ($Ra_L = 1.423\times10^5$).

CONCLUSIONS

The thermal behaviour of three types of local concrete bricks have been studied and analysed numerically in a three-dimensional computational domain under steady-state conditions where one side of the brick was assumed to be hot while the opposite side was assumed to be cold. Temperatures of the heated wall and of the cooled wall were assumed to be constant. The three types of bricks have different external dimensions and different cavity sizes with aspect ratios of 1.167, 1.75, and 3.5 for B20, B15, and B10 respectively. This study showed that the Rayleigh number drastically influenced the flow profile and heat transfer inside the cavity, as well as the thickness of the thermal boundary layer. It was also verified that the Nusselt number is strongly dependent on the aspect ratio, and that this dimensionless variable increases with the increase of this ratio. This study showed that the total heat transfer through B20 is less than those of the other two bricks. Although natural convection heat transfer within B20 cavity is higher, the total heat transfer is still less. This is attributed to the conduction heat transfer which is less in the case of B20. All of this shows that cavity configuration has a remarkable importance for the heat transfer through the brick even for a low temperature difference. This result agrees with statements from previous works.

REFERENCES

[1] Al-Tamimi, A. S., Al-Osta, M. A., Al-Amoudi, O. S. B., Ben-Mansour, R. (2017). Effect of geometry of holes on heat transfer of concrete masonry bricks using numerical analysis, Arab J Sci Eng., Vol. 42, pp. 3733-3749. https://doi.org/10.1007/s13369-017-2482-6.

[2] Bouchair, A. (2008). Steady state theoretical model of fired clay hollow bricks for enhanced external wall thermal insulation, Building and Environment, Vol. 43, No. 10, pp. 1603-1618. https://doi.org/10.1016/j.buildenv.2007.10.005.

[3] Fioretti, R., Principi, P. (2014). Thermal performance of hollow clay brick with low emissivity treatment in surface enclosures, Coatings, Vol. 4, pp. 715-731. https://doi.org/10.3390/coatings4040715.

[4] Svoboda, Z., Kubr, M. (2011). Numerical simulation of heat transfers through hollow bricks in the vertical direction, Journal of Building Physics, Vol. 34, No. 4, pp. 325-350. https://doi.org/10.1177/1744259110388266.

[5] Li, L. P., Wu, Z. G., Li, Z. Y., He, Y. L., Tao, W. Q. (2008). Numerical thermal optimization of the configuration of multi-holed clay bricks used for constructing building walls by the finite volume method, International Journal of Heat and Mass Transfer, Vol. 51, No. 13-14, pp. 3669-3682. https://doi.org/10.1016/j.ijheatmasstransfer.2007.06.008.

[6] Bergman, T. L., Lavine, A. S., Incropera, F. P., Dewitt, D. P. (2011). Fundamentals of heat and mass transfer. 7th ed. Hoboken: Wiley.

[7] White, F. M. (1991). Viscous fluid flow. 2nd Ed. New York: McGraw-Hill.

[8] Cengel, Y. A. (2002). Heat Transfer: A Practical Approach. 2nd ed. McGraw-Hill.

[9] Soylemez, M. S. (1999). On the effective thermal conductivity of building bricks. Building and Environment. Vol. 34, No. 1, pp. 1-5. https://doi.org/10.1016/S0360-1323(98)00002-X.

[10] Wakashima, S., Saitoh, T. S. (2004). Benchmark solutions for natural convection in a cubic cavity using the high-order time–space method, International Journal of Heat and Mass Transfer, Vol. 47, No. 4, pp. 853-864. https://doi.org/10.1016/j.ijheatmasstransfer.2003.08.008.

[11] International Organization for Standardization. ISO 6946: Building components and building elements - Thermal resistance and thermal transmittance -